Received: 10 July 2023 | Revised: 8 September 2023 | Accepted: 9 September 2023

DOI: 10.1002/dvdy.658

PHENOTYPE REPORT

Developmental Dynamics WILEY

Embryonic development in the bonnethead (*Sphyrna tiburo*), a viviparous hammerhead shark

Steven R. Byrum[1,2] | **Bryan S. Frazier**[3] | **R. Dean Grubbs**[4] | **Gavin J. P. Naylor**[2] | **Gareth J. Fraser**[1]

[1]Department of Biology, University of Florida, Gainesville, Florida, USA

[2]Florida Museum of Natural History, Gainesville, Florida, USA

[3]South Carolina Department of Natural Resources, College of Charleston, Charleston, South Carolina, USA

[4]Florida State University Coastal and Marine Laboratory, St. Teresa, Florida, USA

Correspondence
Gareth J. Fraser, Department of Biology, University of Florida, Gainesville, FL, USA.
Email: g.fraser@ufl.edu

Abstract

Background: The hammerhead sharks (family Sphyrnidae) are an immediately recognizable group of sharks due to their unique head shape. Though there has long been an interest in hammerhead development, there are currently no explicit staging tables published for any members of the group. The bonnethead *Sphyrna tiburo* is the smallest member of Sphyrnidae and is abundant in estuarine and nearshore waters in the Gulf of Mexico and Western North Atlantic Ocean. Due to their relative abundance, close proximity to shore, and brief gestation period, it has been possible to collect and document multiple embryonic specimens at progressive stages of development.

Results: We present the first comprehensive embryonic staging series for the Bonnethead, a viviparous hammerhead shark. Our stage series covers a period of development from stages that match the vertebrate phylotypic period, from Stage 23, through stages of morphological divergence to complete development at birth—Stage 35). Notably, we use a variety of techniques to document crucial stages that lead to their extreme craniofacial diversity, resulting in the formation of one of the most distinctive characters of any shark species, the cephalofoil or hammer-like head.

Conclusion: Documenting the development of hard-to-access vertebrates, like this viviparous shark species, offers important information about how new and diverse morphologies arise that otherwise may remain poorly studied. This work will serve as a platform for future comparative developmental research both within sharks and across the phylogeny of vertebrates, underpinning the extreme potential of craniofacial development and morphological diversity in vertebrate animals.

KEYWORDS

craniofacial diversity, evolutionary developmental biology, hammerhead shark, shark embryonic development, staging series

1 | INTRODUCTION

Of all elasmobranchs, sharks in the hammerhead family Sphyrnidae are among the most charismatic and easily recognizable due to their dorsal-ventrally flattened and laterally expanded 'hammer' head, known as the cephalofoil. The major characteristics of this chondrocranium shape include: a secondary supraorbital crest consisting of extended and fused postorbital and preorbital processes just above the eye; laterally extended and dorsoventrally depressed nasal capsules that completely encapsulate the olfactory organs, and from which the preorbital process grows; a depressed and broad medial rostral cartilage flanked by a pair of lateral cartilages, fusing together to form a plate-like rostral node at the anterior end of the snout.[1,2] Within a small group of nine documented species, members of Sphyrnidae exhibit a surprising amount of diversity in terms of body size and cephalofoil morphology; species differ in placement of the nares and eyes, head widths ranging from 18% to 50% of body length, and total lengths ranging from 1 to 6 m.[3] Phylogenetic analyses show a monophyletic group and suggest that the earliest diverging species are those with the most pronounced cephalofoils, which have diminished among more recently derived species such as the bonnethead *Sphyrna tiburo*.[4,5] Interestingly, the two species with the largest and smallest proportional cephalofoils are also among the smallest (the winghead *Eusphyra blochii* and the bonnethead, respectively).

Much of the research on hammerheads has focused on functional morphological aspects of the cephalofoil, investigating possible advantages in electroreception,[6] hydrodynamics,[7] olfaction,[8,9] and binocular vision.[10] However, published research into the embryonic development of this cephalofoil, or any developmental aspect of hammerhead embryology, is limited. Setna and Sarangdhar[11] and Appukuttan[12] observed a small number of winghead embryos at varying advanced stages of development, and Campagno[2] briefly noted the development of supraorbital crests by illustrating cleared and stained embryonic specimens of the scalloped hammerhead, *Sphyrna lewini*.

While aspects of elasmobranch development have long been of interest,[13,14] publications featuring developmental staging series tracking the growth of elasmobranchs have only appeared in the past 30 years. including the small-spotted catshark *Scyliorhinus canicula*,[15,16] the winter skate *Leucoraja ocellata*,[17] the little skate *Leucoraja erinacea*,[18] the Atlantic sharpnose *Rhizoprionodon terraenovae*,[19] the brownbanded bamboo shark *Chiloscyllium punctata*,[20] and the frilled shark *Chlamydoselachus anguineus*.[21] Such work has been particularly valuable for the catshark and little skate, which have become popular models in experimental biology, in part because their eggs can be easily produced, collected, maintained, and observed in captivity,[18,22,23] making them widely used in multiple studies. Developmental staging series allows for the identification of emerging features for experimentation and provide a comparative reference for other published work. For unconventional (or non-classical) model organisms, developmental staging can also aid in identifying the timing and ontogeny of morphological conservation and diversity between species, allowing the understanding of evolutionary changes that have resulted in differences in morphology among species.[24] In this sense, documenting the development of a hammerhead shark is crucial to our understanding of the timing and processes that lead to the elaboration and diversification of the chondrocranium and the unusual cephalofoil. An understanding of the development of these more elusive species offers huge potential in which to uncover the trajectory of morphological novelty and extreme divergence of vertebrate form and function.[25]

A major issue with developing a staging series for sphyrnids (hammerheads) relates to their placental viviparity (placentotrophy), a mode of reproduction found only in five families within Carcharhiniformes.[26] Because viviparous embryos are fully dependent on the mother until birth, specimen collection is lethal, halting observable development into small windows in time. In contrast, oviparous (egg-laying) shark development is easier to observe continuously, and staging series' can be more readily described. To develop a series for a placentotrophic shark requires a relatively abundant species with a manageable size, as was done with the Atlantic sharpnose shark.[19] However, because the family Sphyrnidae includes multiple endangered species and populations,[27] collecting large numbers of embryos is unfeasible for most hammerhead species, in part, leading to the current paucity of developmental information available.

The bonnethead shark is unique among sphyrnids in being one of the smallest species (~1 m in length) and having the proportionally smallest cephalofoil within the family.[5] While populations in the Pacific ocean are of conservation concern, populations in the Gulf of Mexico and western North Atlantic are considered stable as of 2023.[27] Bonnetheads may give birth to up to 18 pups in the late summer to early fall after a short gestation period of 4–5 months; remarkably short for any viviparous elasmobranch.[28–30] Multiple studies have observed the reproductive biology of the bonnethead shark, describing and illustrating placentation and/or late-stage embryonic specimens[31,32] but as with other sphyrnids there is no comprehensive publication of a developmental series. The combination of a short gestation period, stable

Atlantic populations, large litter size, and nearshore availability of pregnant females makes the bonnethead shark the best candidate for observing the development of hammerhead sharks. This study explores the development of the bonnethead shark using recently acquired specimens and museum collections, with a focus on the ontogeny of a novel head shape, unseen in other living vertebrates.

2 | RESULTS

St. 23 (Figure 1A–A″): The first three pharyngeal clefts are open. The first cleft opening is narrowest and open dorsally, second cleft is open widest dorsally while the bottom of the second arch crowds in with first and third arch. The fifth and later sixth pharyngeal pouches are forming, visible by translucence. The mouth opening appears as a thin vertical slit in ventral view. Optic cups appear teardrop shaped with round lens placodes. Olfactory placodes are slightly visible by translucence anterior to the eye. The pineal gland epiphysis is beginning to emerge as a bump in front of the indentation between the forebrain and midbrain. The connection to the yolk sac is broad and takes up much of the ventral side of the body. Tails are curved with a rounded tip.

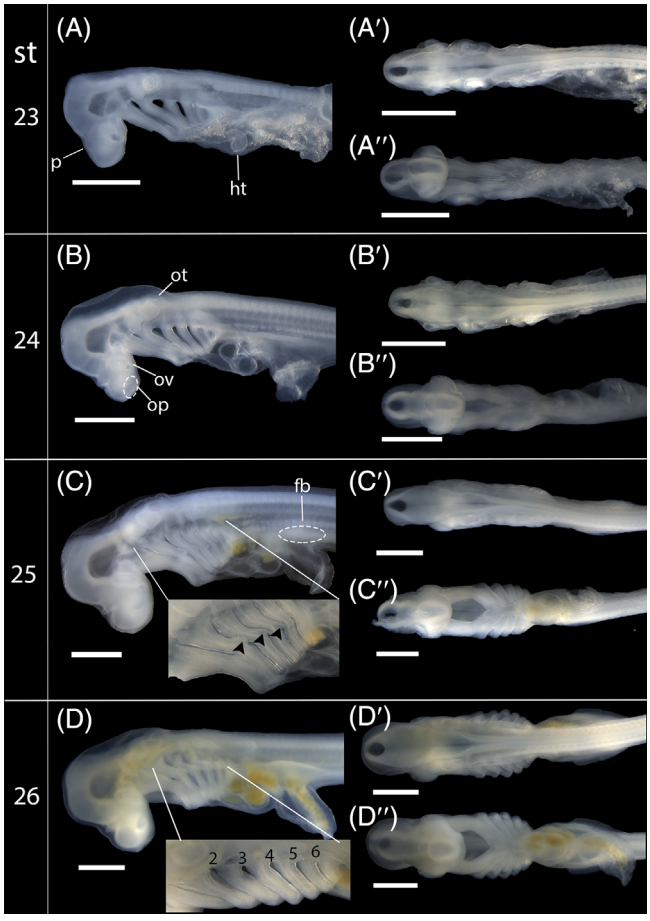

FIGURE 1 Embryos during pharyngeal formation. (A–D, A′–D′, A″–D″) Stages 23–26 in lateral, dorsal (′), and ventral view (″), respectively. Black arrows in C indicate gill buds. Black numbers in D indicate pharyngeal clefts. Scale bars: 1 mm.

St. 24 (Figure 1B–B″): The fourth pharyngeal cleft is opening (Figure 1B). The mouth opening begins to widen in a diamond-like shape (Figure 1B″). Lens develops, pushing into the optic cup. The olfactory placodes begin to depress inwards, forming sunken pits. The endolymphatic ducts begin to form from the otic vesicle above the second pharyngeal cleft. Connection to yolk sac begins to taper and become stalk-like. The cloacal bulge becomes pronounced and visible, partially obscured by folds in lateral view. The tail bends at the cloaca.

St. 25 (Figure 1C–C″): Six gill arches are visible and the fifth pharyngeal cleft is opening (Figure 1C). Gill buds are forming on second, third, and fourth pharyngeal clefts. The endolymphatic ducts have extended and can be seen dorsally along either side of the unclosed neural tube (Figure 1C′). The pectoral fin buds are developing as small crests on either side of the umbilical connection (Figure 1C). The tail curvature is beginning to straighten, no longer bent at the cloaca.

St. 26 (Figure 1D–D″): All six pharyngeal clefts have opened, with arches 2–5 appearing bent at their midpoints in lateral view (Figure 1D). The pectoral fin buds appear as rounded ridges growing perpendicular to the umbilical connection.

St. 27: The nasal opening has sunken, appearing wide and circular in lateral view. The first dorsal, anal, and caudal fins are forming from the median finfold (Figure 3A–A″). Paired pelvic fins appear as lengthening ridges anterior to anal fin fold, smaller than the pectoral fins (Figure 3A″). The paired pectoral fins show possible muscle stripe growth (Figure 3A). Early gill filament buds appear from all pharyngeal clefts. The upper mandibular arch is pressing against the eye.

St. 28 (Figure 2A–A″): The mandibular arches begin to form a bent shape in lateral view (Figure 2A), and a more circular to rectangular appearance in ventral view (Figure 2A′). The nares remain open but are narrowing, taking on an oval appearance. The pectoral and pelvic fins appear as rounded flaps emerging past the midline (Figure 3B,B″). Early fin muscle stripes are present in the pelvic and first dorsal fins (Figure 3B′,B‴). The second dorsal fin bud is beginning to emerge (Figure 3B″). Gill filaments begin to extend past gill arches. Faint pigmentation may begin to appear around the lens of the eyes.

St. 29 (Figure 2B–B″): Eye pigmentation forms an incomplete circle around the eyes (Figure 2B). The gill filaments further elongate partially obscuring the gill arches.

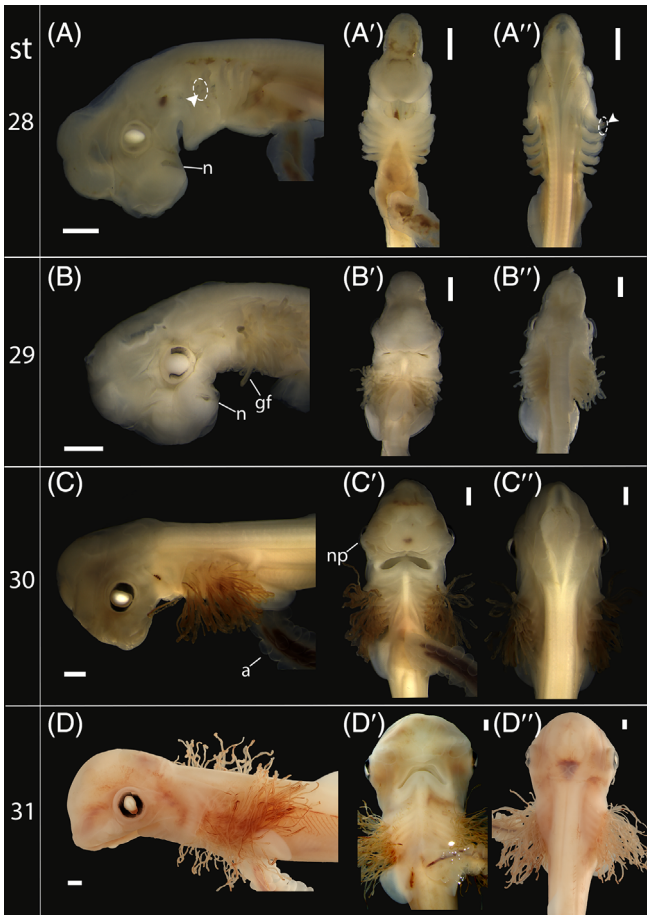

FIGURE 2 Embryos during postpharyngeal formation. (A–D, A′–D′, A″–D″) Stages 28–31 in lateral, ventral (′), and dorsal view (″), respectively. White arrows in (A,A″) indicate emerging gill filaments. Scale bars: 1 mm. a, appendiculae; gf, gill filaments; n, nares; np, nasal process.

The lower mandibular arches continue to push together, and the mouth begins to take an arched shape (Figure 2B′). The nares further narrow into small openings while growing laterally and anterior to the eyes, partially obstructing the eyes in ventral view of some specimens (Figure 2B). Muscle stripes appear on the developing second dorsal fin, and both the second dorsal and anal fins have yet to fully separate from the fin fold (Figure 3C–C‴).

St. 30 (Figure 2C–C″): The eyes are completely encircled by black pigment. Early rostral expansion begins with a broadening of the head region anterior to the nasal organs, while distinct outgrowth of the nasal organs continues laterally, the nares now facing ventral to the head (Figure 2C′). Alcian blue-stained sections show cartilage surrounding the olfactory organ (Figure 4A). Mesencephalon is becoming less prominent than previous stages as a result of this new growth. Small gill filaments begin to emerge from the spiracular (first) clefts (Figure 2C). Appendiculae begin to form as small buds on the umbilical stalk. All fins are now distinct, with only the caudal fin showing remnants of a fin fold (Figure 3D–D‴). Developing claspers are visible in males as small expansions of the pelvic fin posterior, which meet closer together in comparison to females. Developing ampullae of lorenzini are present along the rostrum.

St. 31 (Figure 2D–D″): The developing rostrum is broader and rounded in both ventral and dorsal view, with anterior expansion making the rostrum almost on par with the mesencephalon as the anterior-most point of the embryo. The first dorsal fin is triangular with a posterior curve, and an inner margin appears as a small notch (Figure 3E′). Alcian blue-stained sections show rostral cartilage outgrowth (Figure 4B). Computed tomography (CT) data and clear and stain imaging show visible chondrification of jaws, hyoid, gill arches, and posterior base of the chondrocranium (Figure 5A′,A″). Appendiculae project from the umbilical as finger-like projections.

St. 32 (Figure 6A–A″): The angle formed by the anterior and the dorsal surface of the head becomes increasingly obtuse as rostral growth and lateral expansion continue. The rostrum becomes the anterior-most point of the embryo, establishing the characteristic Bonnethead cephalofoil shape (Figure 6A); CT scanning of a 90 mm embryo shows the medial rostral cartilage is nearly fully formed, and the preorbitals and postorbitals have met and fused (Figure 5B). Taste buds are distributed throughout the basihyal and pharyngeal arches. Lower jaw histology shows early dental lamina development and the first sign of tooth development (Figure 7A′). New tooth replacements will emerge from the free end of the dental lamina, and are added to the tooth family, lingual to the first tooth germ (highlighted in Figure 7A′–C′). Gill filaments begin to recede until only a few filaments protrude from the posterior gills.

St. 33 (Figure 6B–B″): A brief stage in which the gill filaments have completely receded. Denticle placodes begin to appear on the ventral body surface and sides of tail (Figure 7B″). Developing embryos up to this point have been pale but are now beginning to show specks of pigment on the dorsal side of the body. Tooth germs increase in number from one to two and remain embedded in the epithelial dental lamina. The first tooth continues development and begins the process of morphogenesis and initial mineralization (Figure 7B,B′).

St. 34 (Figure 5C–C″): Dermal denticles are forming and spreading across the body along with gray pigmentation on the dorsal side, with denticles spreading to the dorsal side of the head and fins last. Figure 7C″ shows denticles on the ventral side of the lower jaw. Dark gray pigmentation appears along the leading edge of the caudal fin and the first and second dorsal fins. The first dorsal fin has proportionally increased in size with respect to the rest of the body in comparison to the previous stage. There are several generations of teeth within the dental

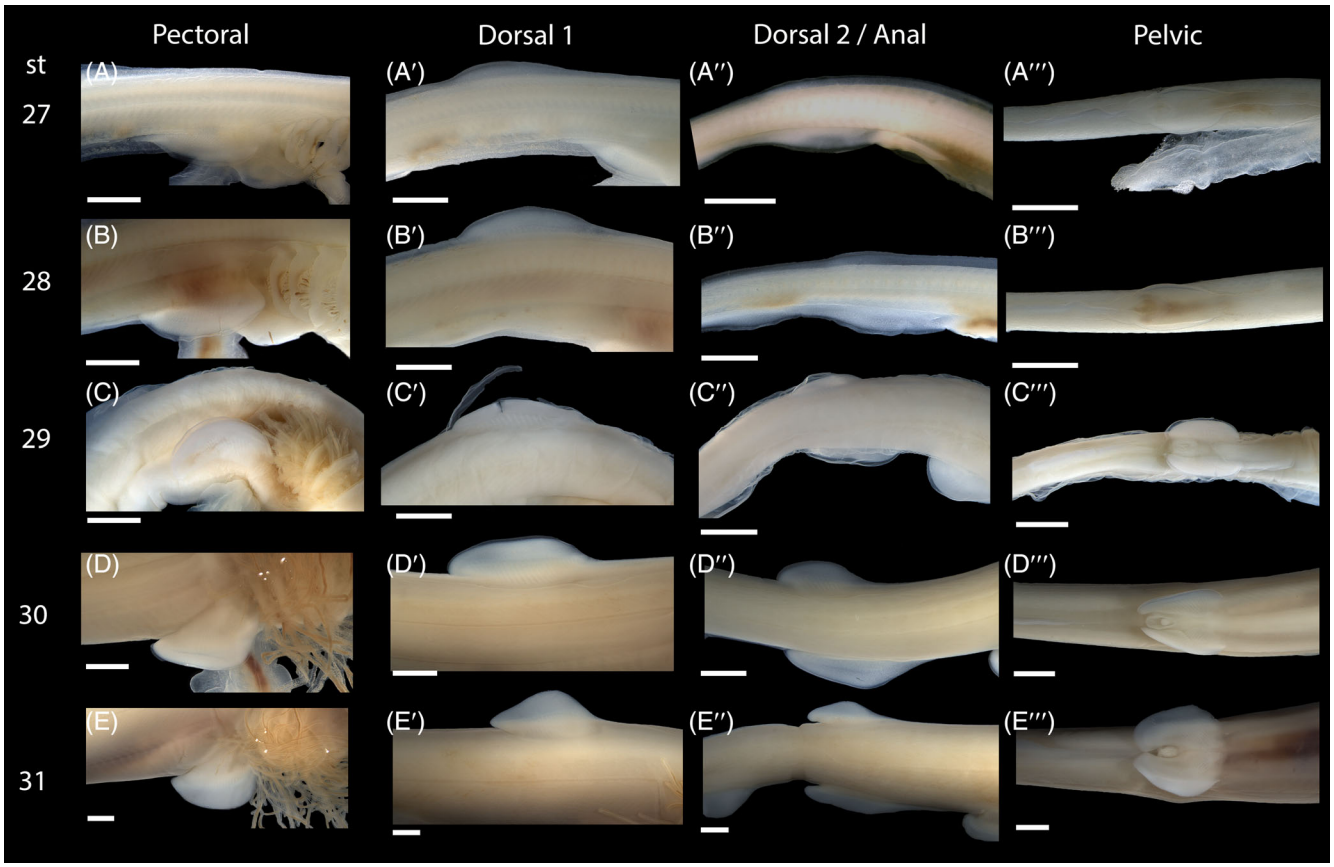

FIGURE 3 Fin development during post-pharyngeal formation. The pectoral fins, dorsal fins, anal fins, and pelvic fins of stages 27 (A–A″), 28 (B–B″), 29 (C–C″), 30 (D–D″), and 31 (E–E″). Scale bars: 1 mm.

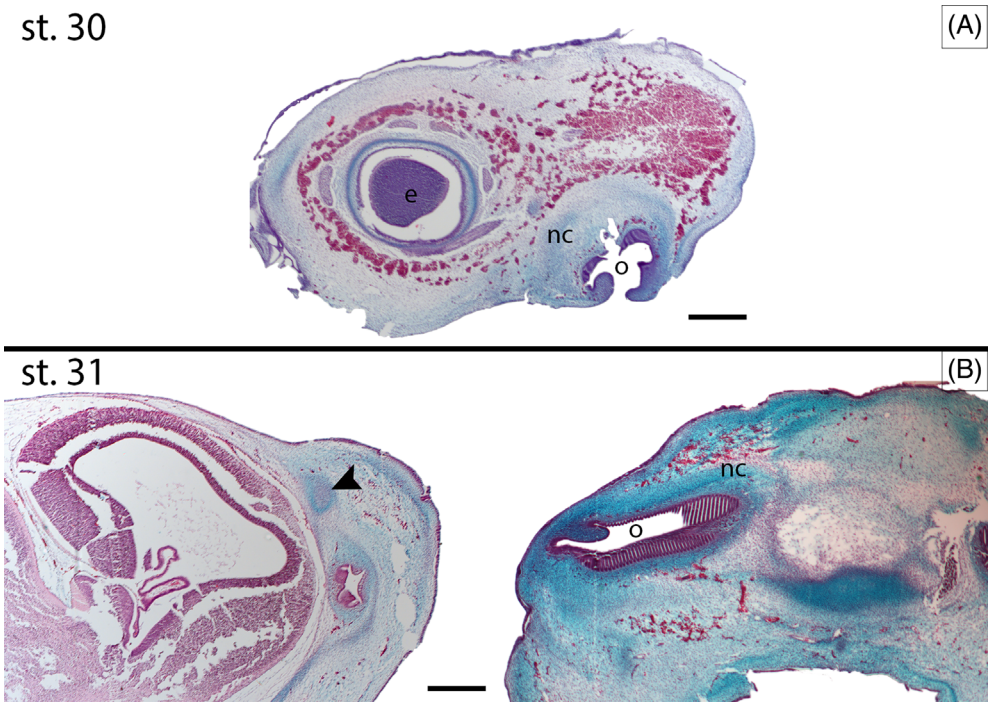

FIGURE 4 Hemotoxylin & Eosin (H&E) and alcian blue-stained histological sections of Stage 30 (A) and Stage 31 (B) bonnethead embryos in sagittal and transverse (B only) view at 2.5× magnification. Alcian blue stain shows cartilage surrounding the olfactory organ in both stages, as well as rostral growth in Stage 31. Scale bars: 500 μm. arrowhead, area of rostral growth; e, eye; nc, nasal capsule; o, olfactory organ.

lamina (Figure 7C,C′). Lower jaw histology reveals three generations of teeth undergoing morphogenesis and maturation prior to eruption (still enveloped within the epithelail dental lamina). New tooth replacements will emerge from the free end of the dental lamina (successional lamina).

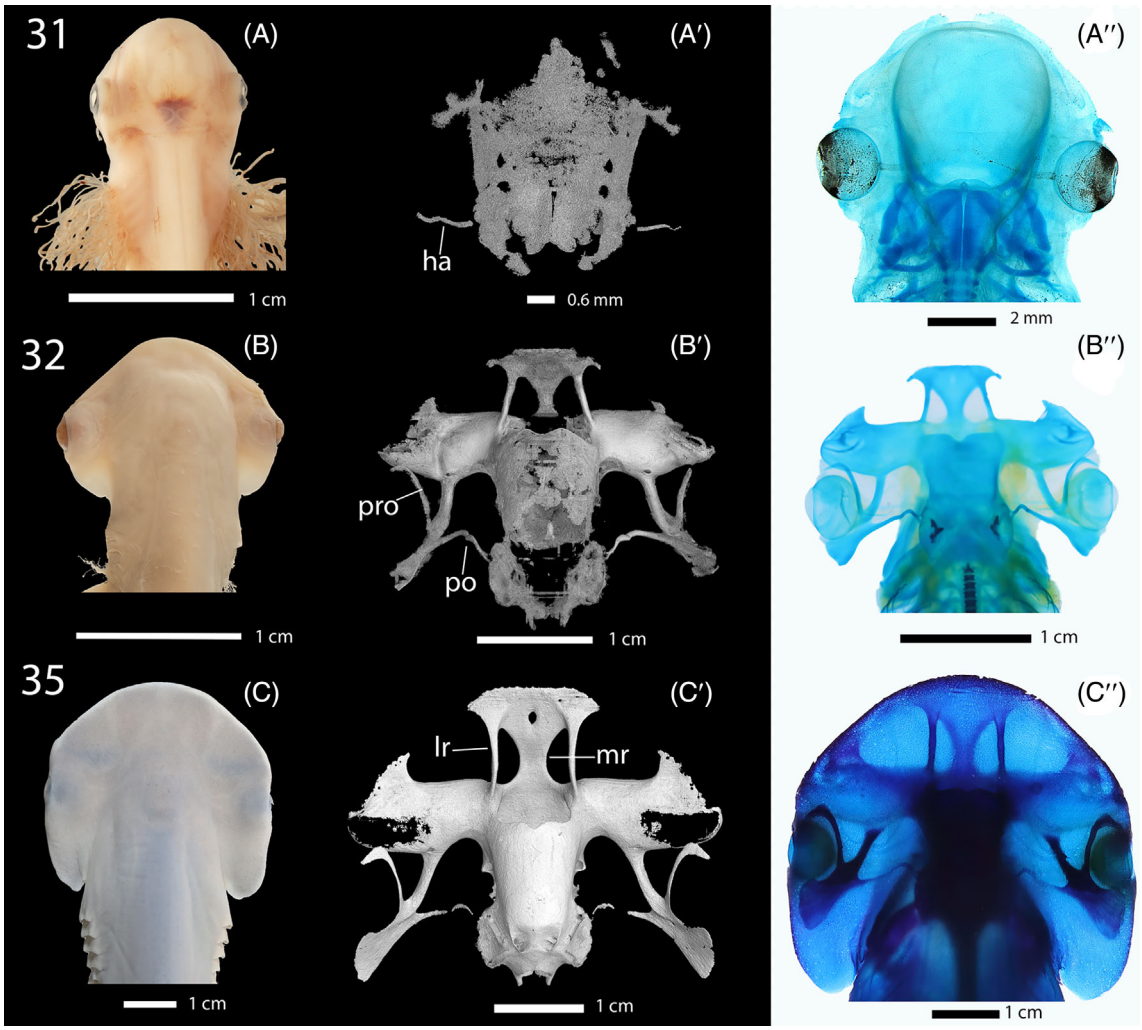

FIGURE 5 Computed tomography imaging, clear and stained images of Stages 31 (A–A″), 32 (B–B″), and 35 (C–C″) bonnethead embryos in dorsal view. By Stage 32, preorbital and postorbital processes fuse as the bonnethead cephalofoil is established.

St. 35 (Figure 8): General isometric body growth until birth. Denticles have completely covered the body. Embryos at this point are fully pigmented and have acquired the appearance of neonate juvenile. Cleared and stained imaging and CT imaging show the chondrocranium is fully developed, with secondary calcification occurring in the jaw, vertebra, brain case, lateral rostral cartilage, and preorbital (Figure 5C″), appearing as darkened parts of the chondrocranium. At this stage, teeth of the first generation erupt and the dentition is fully functional.

3 | DISCUSSION

This staging series follows a sequential numbering system following staging tables developed for the catshark,[15] bamboo shark,[20] and ghost shark.[33] Up to postpharyngeal development, the bonnethead embryo shares many similarities with the corresponding stages of small-spotted catshark; allometric plots of nasal and interorbital width measurements versus total length of Stage 28 bonnethead embryos appear comparable to those of Stage 28 catsharks (Figures 9 and 10). The most dramatic morphological divergence between the two species appears to begin at bonnethead Stage 30, when the lateral expansion of the bonnethead olfactory organs becomes prominent. The extending organs and outgrowth of rostral cartilage form a broad, rounded shape to the chondrocranium. As the embryos of both species mature, the physical differences in morphology become more prominent; the olfactory organs of hammerheads and related families end in extended peduncles that connect the organs to the telencephalon. The peduncle of the catshark is comparatively reduced, and the olfactory organs are physically closer in attachment to the telencephalon. Scyliorhinids such as the small-spotted catshark (*Scyliorhinus canicula*) are oviparous and have unadorned yolk

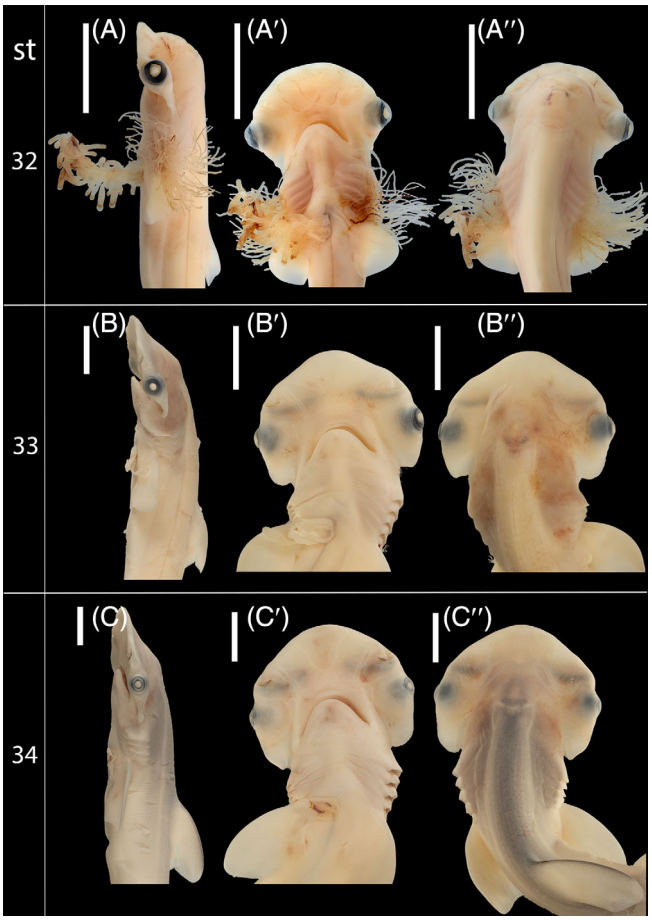

FIGURE 6 Bonnethead shark embryos during late embryonic development. (A–C, A′–C′, A–C″) Stages 32–34 in lateral, ventral (′), and dorsal view (″), respectively. Scale bars: 1 cm.

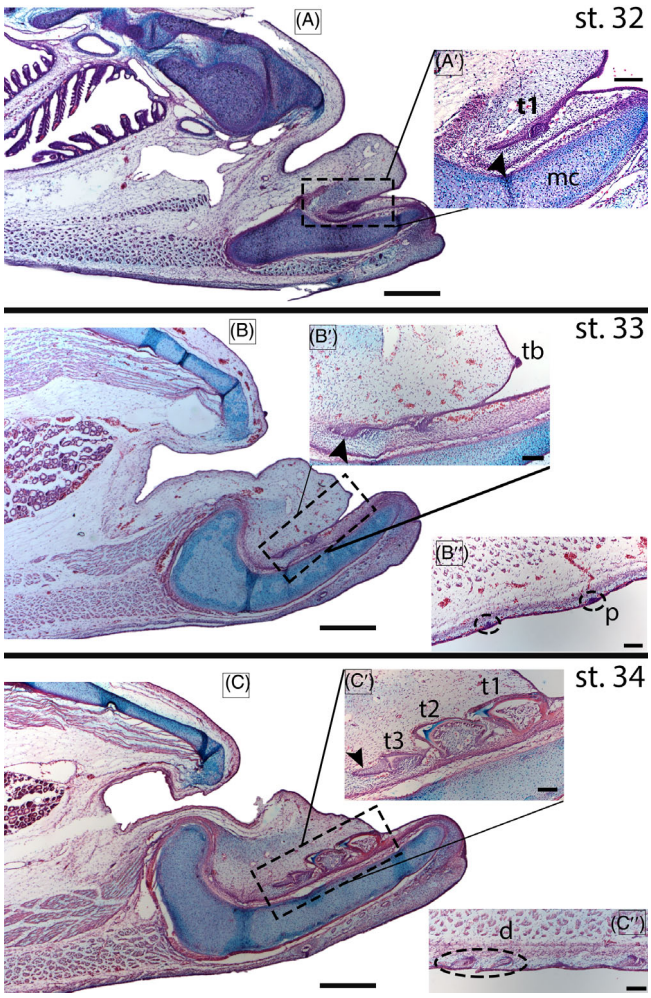

FIGURE 7 H&E and alcian blue-stained histological sections of of lower jaw in sagittal view at Stages 32 (A–A′), 33 (B–B″), and 34 (C–C″). (B″,C″) Presence of skin denticle development. (A–C) at 2.5× magnification, and all insets at 10× magnification. Scale bars: 500 μm (A–C); 100 μm (all insets). Black arrowhead, successional lamina; d, denticle; mc, Meckel's cartilage; p, denticle placode; t1, tooth 1; tb, taste bud.

stalks; however, Stage 30 bonnethead specimens begin to develop appendiculae, appearing as knobs on the umbilical stalk, at a similar size range to their appearance in the carcharhinid Atlantic sharpnose shark.[19] These appendiculae remain present until birth, possibly as a source of nutrient absorption and/or gas exchange. Gill filament reduction concludes rather quickly, as individuals within litters of equivalent body size may show the presence or absence of filaments as they recede into the gill arches. This reduction seems to occur slightly later than other species. Ballard et al.[15] and Castro and Wourms[19] both note the reduction of gill filaments in the small-spotted catshark and the Atlantic sharpnose at a point in which the vestiges of the fin-fold have regressed and rostral outgrowth proceed.

Model elasmobranchs such as *Scyliorhinus* and *Leucoraja* are known to begin denticle patterning with caudal denticles restricted to the tail, and two initial dorsal rows followed by more general body denticle distribution, an adaptation thought to aid in movement during hatching and/or promote circulation within the egg case during oviparous development.[34,35] This denticle patterning is not always present in other elasmobranchs, especially in species with alternative modes of gestation/incubation. In the bonnethead, initial denticle placodes seem to first appear on the lower ventral side of the embryo before spreading across the dorsal body, without the same initial denticle rows observed in oviparous sharks, for example, the small-spotted catshark.[36,37] In addition, while internal oral denticles are present in many elasmobranch species, little is known about developmental timing of the appearance of these oral denticles or how they may differ from skin denticles, as this trait is not present in the well-studied small-spotted catshark. After the point of denticle distribution and coloration, the bonnethead experiences more generalized allometric

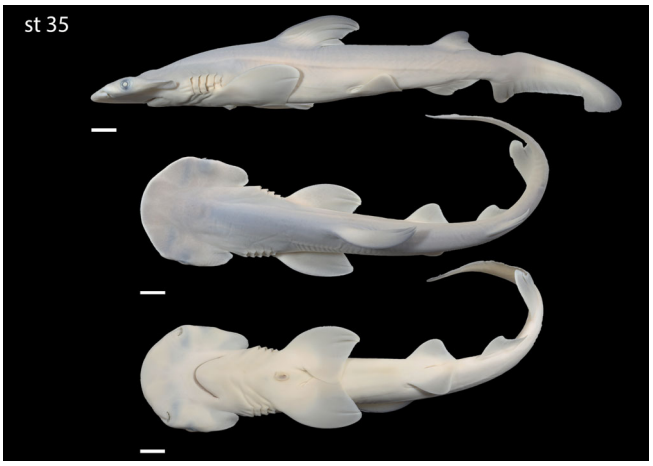

FIGURE 8 Dorsal, ventral, lateral views of the final embryonic stage (st. 35) bonnethead shark. Scale bars: 1 cm.

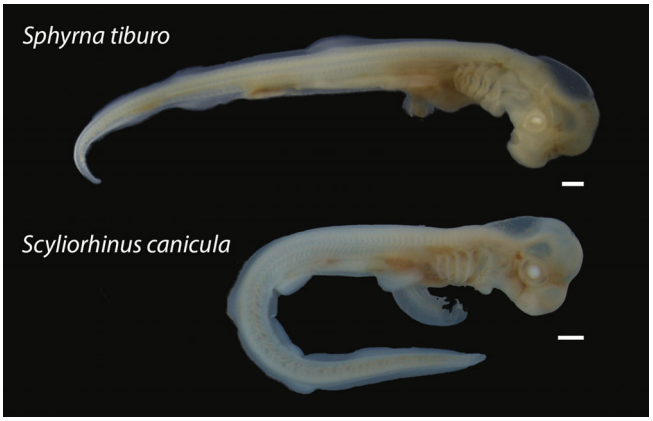

FIGURE 9 Comparative Stage 28 embryos of the bonnethead (*Sphyrna tiburo*; top) and small-spotted catshark (*Scyliorhinus canicula*; bottom) showing the similarity of the stage in divergent shark species (note that Scyliorhinus tail is bent due to specimen fixation issues).

growth, and upon birth will resemble a miniature version of the adult.

An illustration by Campagno[2] shows progressive stages of supraorbital crest development in three scalloped hammerhead (*Sphyrna lewini*) specimens. The preorbital and postorbital processes grow separately, as in carcharhinids, and migrate towards the eye, eventually meeting and fusing together with a clear line of fusion. Upon Stage 32, CT data show the orbital processes have met and fused, with a clear line of fusion (Figure 5B′). Scyliorhinid orbitals are fused to the rest of the main chondrocranium, whereas sphyrnid preorbitals are connected to the nasal capsule and fused with an elongated postorbital, distal from the rest of the chondrocranium. This condition also differs from related carcharhiniform families, which do not exhibit any fusion of the orbitals.

The comparatively reduced cephalofoil of the bonnethead raises questions about the development of other hammerhead species with proportionally larger heads. While initial cephalofoil development may be similar within the group, the differences in timing and growth rate between species are uncertain. Describing a 43 mm winghead embryo, Setna and Sarangdhar[11] noted lateral projections with slit-like nares anterior to the eye. Late-stage embryos of the same species described by Appukkutan[12] shows the characteristic cephalofoil fully formed with the eyes and nasal capsule folded backwards within the uterus, straightening out just after birth as described by Campagno.[2]

Interestingly, later-stage specimens of equivalent stages from different years showed notable differences in size. For example, Stage 33 specimens collected in 2021 range in total body length from ∼100 to 125 mm but range from ∼88 to 100 mm from the same locality the following year; Stage 34 specimens ranged from 138 to 155 mm total body length in 2021, but 99–109 mm in 2022. In addition, specimens captured in Florida in 2021 were more developmentally advanced than specimens captured in South Carolina at similar dates. The difference in embryo size may relate to slight shifts in water temperature affecting growth, as higher temperatures have been documented to negatively impact embryonic growth and metabolism in other species.[38] The difference in developmental timing among localities have been previously observed, and may relate to differences in latitude, and thus differences in seasons and timing of pregnancy in adult females.[29,30,39] These differences, particularly those of embryo size, illustrate the importance of characterizing stages by the appearance of morphological characters as opposed to physical measurements.

Due to the nature of collecting embryos from a viviparous species in the wild, a complete staging series starting from fertilization is a difficult task. Embryonic specimens must come from different sources and are not observable until the mother is sacrificed, which makes obtaining sequential stages more challenging. This usually leads to a smaller number of embryos for collection, which makes accounting for possible heterochrony in developmental stages more difficult. Nevertheless, this staging series covers a wide span of bonnethead shark development, from early pharyngeal development to cephalofoil formation, up to birth, and represents the first such series of any hammerhead shark species. The development of species that present more extreme phenotypes offers a better understanding of not only the timing of developmental and morphological divergence (heterochrony) but aids our overall appreciation of developmental conservation (e.g., the phylotypic period of vertebrate development) and the changes that occur from these more common

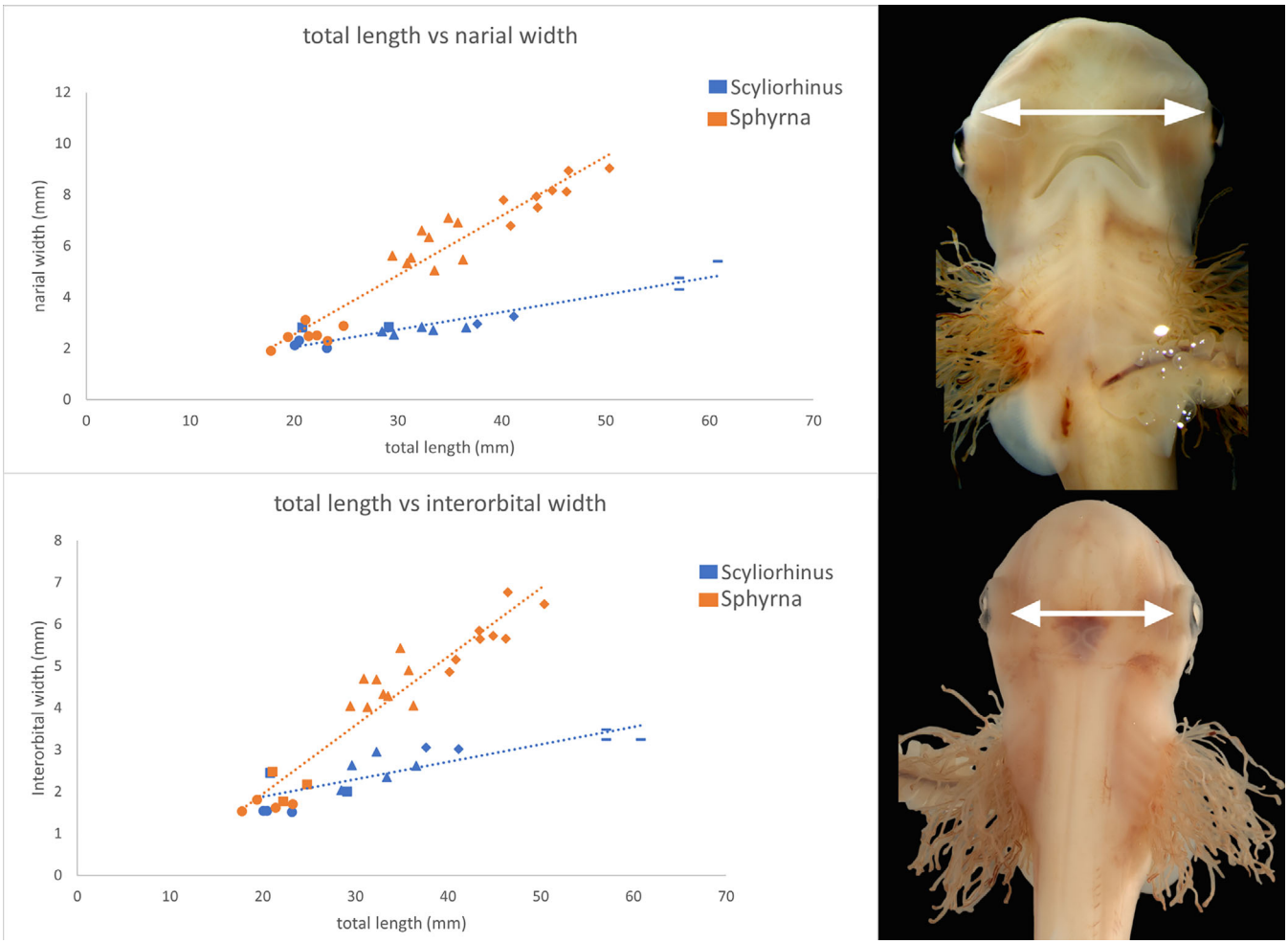

FIGURE 10 Allometric plots showing total length versus orbital width and narial width in early Stages (28–31) of *Sphyrna tiburo* and *Scyliorhinus canicula*. Circles: St. 28, Squares: St. 29, Triangles: St. 30, and Bars: St. 32.

periods of phyla-specific development, in keeping with the hour-glass hypothesis of development.[25,40,41] Access to lesser-known models that present extreme developmental and morphological divergences, like the bonnethead, provides unrivaled comparative insights into how the vertebrate bauplan can shift so dramatically during ontogeny. Our work helps to offer a unique perspective on the potential extreme outcomes and constraints on vertebrate evolutionary trajectories, and ultimately why these more extreme phenotypes are relatively rare in nature.

4 | EXPERIMENTAL PROCEDURES

Adult sharks and embryos were obtained via gillnet during biological surveys off North Edisto Island, South Carolina (32°37′N, 80°15′W) in partnership with the South Carolina Department of Natural Resources; and Florida's Gulf coast from St. George Sound (29°53′N, 84°30′W) to near Anclote Keys (28°14′N, 82°46′W) by the Florida State University Coastal and Marine Lab. Adult females were euthanized via severing of spinal column. Embryos were collected from uteri and fixed with 4% paraformaldehyde in phosphate buffered saline (PBS) at 4°C overnight, followed by dehydration using a series of PBS/ethanol (75% PBS/25% EtOH, 50%/50%, 25% PBS/75% EtOH, 100% EtOH), and stored in 100% ethanol at −20°C. Embryos were rehydrated in PBS for photography. Images were taken in dorsal, lateral, and ventral views using Leica stereoscope and Canon EOS R, and Z-stacking was conducted using LAS X software and Helicon Focus Software, respectively. To compare early cephalofoil development with more standard chondrocranial growth in other elasmobranchs, 25 imaged specimens of bonnethead and 15 specimens of small-spotted catshark were measured for interorbital width, narial width, and total body length using ImageJ and used in allometric plots. Measurement parameters were based on Grunow et al. (2022). For CT scanning specimens were

prepared in 0.3% phosphotungstic acid (PTA) in 70% ethanol for 14 days or 1% ruthenium red (see Ref. [42]) as contrasting staining agents. Two PTA specimens (Stages 32 and 35) were scanned at 70 kV and 260 μA, and a ruthenium red specimen (Stage 31) was scanned at 100 kV and 80 μA. Histological sections were produced by embedding tissue in paraffin, cutting 8–10 μm sections on a Leica microtome and staining with hemotoxylin, 1% eosin in water, and 0.1% alcian blue in 3% acetic acid to stain nuclei, extracellular material, and cartilage, respectively. Two Stage 31 embryos, one Stage 32 lower jaw, one Stage 33 lower jaw, and one Stage 34 lower jaw were used. Whole mount cleared and stained specimens were prepared using a modified procedure by Dingerkus and Uhler[43] using 0.2 g Alcian blue per 100 mL of 30% acetic acid in ethanol for cartilage staining, 1% trypsin in 30% saturated sodium borate in water for tissue digestion, 0.5% potassium hydroxide (KOH) for bleaching, 0.2 g alizarin red per 100 mL 0.5% potassium hydroxide in water for mineralized tissue, and a graded series of 3:1, 1:1, 3:1 of 0.5% KOH:glycerol, followed by 100% glycerol for specimen clearing (one Stage 31, one Stage 32, and one Stage 35 specimen were used. All field collections were carried out under necessary state, and university-specific protocols: Collection of specimens in South Carolina was performed under SCDNR Scientific Permit no. 2212. All Florida field collections were carried out under Florida Fish and Wildlife Conservation Commission Special Activities License SAL-1092 and in accordance with Florida State University Animal Care and Use Committee (ACUC) protocol PROTO202000020 (Table 1).

TABLE 1 Specimens and collection sites of Sphyrna tiburo observed in this study.

Date	Location	Coordinates	No. embryos	Stage
May 31, 1976	Biscayne Bay, Florida	25°31′N, 80°13′W	1	32
June 16, 2020	Florida	29°08′N, 82°55′W	15	34
August 19, 2020	Florida	29°41′N, 85°01′W	7	35
June 1, 2021	Florida	29°50′N, 84°38′W	9	30
June 2, 2021	North Edisto, South Carolina	32°37′N, 80°15′W	9	23–26
June 15, 2021	Florida	29°06′N, 82°55′W	6	32
June 16, 2021	North Edisto, South Carolina	32°37′N, 80°15′W	5	27,28
June 17, 2021	North Edisto, South Carolina	32°37′N, 80°15′W	6	30
June 23, 2021	Florida	29°27′N, 83°23′W	9	32
June 26, 2021	North Edisto, South Carolina	32°37′N, 80°15′W	12	31
July 2, 2021	North Edisto, South Carolina	32°37′N, 80°15′W	1	32
July 12, 2021	Florida	28°16′N, 82°46′W	8	34
July 26, 2021	North Edisto, South Carolina	32°37′N, 80°15′W	5	33
August 2, 2021	North Edisto, South Carolina	32°37′N, 80°15′W	4	34
August 2, 2021	North Edisto, South Carolina	32°37′N, 80°15′W	3	34
August 11, 2021	North Edisto, South Carolina	32°37′N, 80°15′W	8	34
September 8, 2021	North Edisto, South Carolina	32°37′N, 80°15′W	2	35
June 7, 2022	North Edisto, South Carolina	32°37′N, 80°15′W	3	28
June 7, 2022	North Edisto, South Carolina	32°37′N, 80°15′W	6	29
July 20, 2022	North Edisto, South Carolina	32°37′N, 80°15′W	6	34
July 22, 2022	North Edisto, South Carolina	32°37′N, 80°15′W	7	34
July 8, 2022	North Edisto, South Carolina	32°37′N, 80°15′W	6	32
July 8, 2022	North Edisto, South Carolina	32°37′N, 80°15′W	10	32
August 5, 2022	North Edisto, South Carolina	32°37′N, 80°15′W	7	35
August 5, 2022	North Edisto, South Carolina	32°37′N, 80°15′W	8	35
August 8, 2022	North Edisto, South Carolina	32°37′N, 80°15′W	2	35
August 8, 2022	North Edisto, South Carolina	32°37′N, 80°15′W	5	35
August 17, 2022	North Edisto, South Carolina	32°37′N, 80°15′W	7	35

Note: Embryos listed by date captured with corresponding location, number of embryos, and determined stages.

ACKNOWLEDGMENTS

We thank the members of the Fraser, Naylor, Grubbs and Frazier labs for their support and assistance with collection, specifically Wesley Dillard, Ella Nicklin, Lei Yang, Joe Miguez, Adrian Lee, Karly Cohen, and Ashley Galloway. Thanks to Zach Randall and Ed Stanley for their invaluable support with CT imaging. We are also grateful for the reviewers' constructive comments on previous versions.

ORCID

Steven R. Byrum https://orcid.org/0000-0003-4147-7422
Gareth J. Fraser https://orcid.org/0000-0002-7376-0962

REFERENCES

1. Gilbert CR. A revision of the hammerhead sharks (family Sphyrnidae). *Proc US Natl Mus*. 1967;119(3539):1-88. doi:10.5479/si.00963801.119-3539.1
2. Compagno LJV. *Sharks of the Order Carcharhiniformes*. Princeton University Press; 1988.
3. Mara KR, Motta PJ, Martin AP, Hueter RE. Constructional morphology within the head of hammerhead sharks (sphyrnidae): cranial morphology in hammerhead sharks. *J Morph*. 2015;276(5):526-539. doi:10.1002/jmor.20362
4. Naylor GJP. The phylogenetic relationships among requiem and hammerhead sharks: inferring phylogeny when thousands of Most parsimonious trees result. *Cladistics*. 1992;8(4):295-318. doi:10.1111/j.1096-0031.1992.tb00073.x
5. Lim DD, Motta P, Mara K, Martin AP. Phylogeny of hammerhead sharks (family Sphyrnidae) inferred from mitochondrial and nuclear genes. *Mol Phylogenet Evol*. 2010;55(2):572-579. doi:10.1016/j.ympev.2010.01.037
6. Kajiura SM, Holland KN. Electroreception in juvenile scalloped hammerhead and sandbar sharks. *J Exp Biol*. 2002;205(23):3609-3621. doi:10.1242/jeb.205.23.3609
7. Gaylord MK, Blades EL, Parsons GR. A hydrodynamics assessment of the hammerhead shark cephalofoil. *Sci Rep*. 2020;10(1):14495. doi:10.1038/s41598-020-71472-2
8. Kajiura SM, Forni JB, Summers AP. Olfactory morphology of carcharhinid and sphyrnid sharks: does the cephalofoil confer a sensory advantage? *J Morphol*. 2005;264(3):253-263. doi:10.1002/jmor.10208
9. Rygg AD, Cox JPL, Abel R, Webb AG, Smith NB, Craven BA. A computational study of the hydrodynamics in the nasal region of a hammerhead shark (*Sphyrna tudes*): implications for olfaction. *PLoS One*. 2013;8(3):e59783. doi:10.1371/journal.pone.0059783
10. McComb DM, Tricas TC, Kajiura SM. Enhanced visual fields in hammerhead sharks. *J Exp Biol*. 2009;212(24):4010-4018. doi:10.1242/jeb.032615
11. Setna S, Sarangdhar P. Studies on the development of some Bombay elasmobranchs. *Rec Ind Mus*. 1949;47(12):203-216.
12. Appukuttan KK. Studies on the developmental stages of hammerhead shark Sphyrna (eusphyrna) blochii from the Gulf of Mannar. *Indian J Fish*. 1978;25:41-52.
13. De Beer GR. The development of the skull of Scyllium (Scyliorhinus) canicula L. *J Cell Sci*. 1931;2(296):591-646.
14. El-Toubi MR. The development of the chondrocranium of the spiny dogfish, Acanthias vulgaris (Squalus acanthias). Part I. Neurocranium, mandibular and hyoid arches. *J Morphol*. 1949;84(2):227-279. doi:10.1002/jmor.1050840204
15. Ballard WW, Mellinger J, Lechenault H. A series of normal stages for development of *Scyliorhinus canicula*, the lesser spotted dogfish(Chondrichthyes: Scyliorhinidae). *J Exp Zool*. 1993;267(3):318-336. doi:10.1002/jez.1402670309
16. Grunow B, Reismann T, Moritz T. Pre-hatching ontogenetic changes of morphological characters of small-spotted catshark (*Scyliorhinus canicula*). *Fishes*. 2022;7(3):100. doi:10.3390/fishes7030100
17. Maxwell EE, Fröbisch NB, Heppleston AC. Variability and conservation in late chondrichthyan development: ontogeny of the winter skate (*Leucoraja ocellata*). *Anat Rec*. 2008;291(9):1079-1087. doi:10.1002/ar.20719
18. Gillis JA, Bennett S, Criswell KE, et al. Big insight from the little skate: Leucoraja erinacea as a developmental model system. *Curr Top Dev Biol*. 2022;147:595-630. doi:10.1016/bs.ctdb.2021.12.016
19. Castro JI, Wourms JP. Reproduction, placentation, and embryonic development of the Atlantic sharpnose shark, Rhizoprionodon terraenovae. *J Morphol*. 1993;218(3):257-280. doi:10.1002/jmor.1052180304
20. Onimaru K, Motone F, Kiyatake I, Nishida K, Kuraku S. A staging table for the embryonic development of the brown-banded bamboo shark (Chiloscyllium punctatum): bamboo shark development. *Dev Dyn*. 2018;247(5):712-723. doi:10.1002/dvdy.24623
21. Lopez-Romero FA, Klimpfinger C, Tanaka S, Kriwet J. Growth trajectories of prenatal embryos of the deep-sea shark Chlamydoselachus anguineus (Chondrichthyes). *J Fish Biol*. 2020;97(1):212-224. doi:10.1111/jfb.14352
22. Coolen M, Menuet A, Chassoux D, et al. The Dogfish *Scyliorhinus canicula*: a reference in jawed vertebrates. *Cold Spring Harb Protoc*. 2008;2008(12):pdb-emo111. doi:10.1101/pdb.emo111
23. Godard BG, Mazan S. Early patterning in a chondrichthyan model, the small spotted dogfish: towards the gnathostome ancestral state. *J Anat*. 2013;222(1):56-66. doi:10.1111/j.1469-7580.2012.01552.x
24. López-Romero FA, Berio F, Abed-Navandi D, Kriwet J. Early shape divergence of developmental trajectories in the jaw of galeomorph sharks. *Front Zool*. 2022;19(1):7. doi:10.1186/s12983-022-00452-1
25. Richardson MK. Heterochrony and the phylotypic period. *Dev Biol*. 1995;172(2):412-421. doi:10.1006/dbio.1995.8041
26. Buddle AL, Van Dyke JU, Thompson MB, Simpfendorfer CA, Whittington CM. Evolution of placentotrophy: using viviparous sharks as a model to understand vertebrate placental evolution. *Mar Freshw Res*. 2019;70(7):908. doi:10.1071/MF18076
27. Pollom R, Carlson J, Charvet P, et al. *Sphyrna tiburo*. The IUCN Red List of Threatened Species 2021: e.T39387A205765567. Published online July 2, 2019 2023. doi:10.2305/IUCN.UK.2021-3.RLTS.T39387A205765567.en
28. Manire CA, Rasmussen LEL, Hess DL, Hueter RE. Serum steroid hormones and the reproductive cycle of the female Bonnethead shark, *Sphyrna tiburo*. *Gen Comp Endocrinol*. 1995;97(3):366-376. doi:10.1006/gcen.1995.1036
29. Lombardi-Carlson LA, Cortés E, Parsons GR, Manire CA. Latitudinal variation in life-history traits of bonnethead sharks, *Sphyrna tiburo*, (Carcharhiniformes: Sphyrnidae) from the

eastern Gulf of Mexico. *Mar Freshw Res*. 2003;54(7):875. doi:10.1071/MF03023
30. Gonzalez De Acevedo M, Frazier BS, Belcher C, Gelsleichter J. Reproductive cycle and fecundity of the bonnethead *Sphyrna tiburo* L. from the Northwest Atlantic Ocean. *J Fish Biol*. 2020;97(6):1733-1747. doi:10.1111/jfb.14537
31. Leuckart FS. *Untersuchungen Über Die Äusseren Kiemen Der Embryonen von Rochen Und Hayen: Ein Beitrag Zur Entwicklungsgeschichte Der Der Abtheilung Der Knorpelfische Angehörenden Plagiostomen*. LF Rieger; 1836.
32. Schlernitzauer DA, Gilbert PW. Placentation and associated aspects of gestation in the bonnethead shark, Sphyrna tiburo. *J Morphol*. 1966;120(3):219-231. doi:10.1002/jmor.1051200302
33. Didier DA, LeClair EE, Vanbuskirk DR. Embryonic staging and external features of development of the Chimaeroid fish, *Callorhinchus milii* (Holocephali, Callorhinchidae). *J Morphol*. 1998;236(1):25-47.
34. Grover CA. Juvenile denticles of the swell shark *Cephaloscyllium ventriosum*: function in hatching. *Can J Zool*. 1974;52(3):359-363. doi:10.1139/z74-043
35. Johanson Z, Smith MM, Joss JMP. Early scale development in *Heterodontus* (Heterodontiformes; Chondrichthyes): a novel chondrichthyan scale pattern. *Acta Zool*. 2007;88(3):249-256. doi:10.1111/j.1463-6395.2007.00276.x
36. Cooper RL, Thiery AP, Fletcher AG, Delbarre DJ, Rasch LJ, Fraser GJ. An ancient Turing-like patterning mechanism regulates skin denticle development in sharks. *Sci Adv*. 2018;4(11). doi:10.1126/sciadv.aau5484
37. Cooper RL, Nicklin EF, Rasch LJ, Fraser GJ. Teeth outside the mouth: The evolution and development of shark denticles. *Evol Dev*. 2023;25(1):54–72. doi:10.1111/ede.12427
38. Wheeler CR, Rummer JL, Bailey B, Lockwood J, Vance S, Mandelman JW. Future thermal regimes for epaulette sharks (*Hemiscyllium ocellatum*): growth and metabolic performance cease to be optimal. *Sci Rep*. 2021;11(1):454. doi:10.1038/s41598-020-79953-0
39. Parsons GR. Geographic variation in reproduction between two populations of the bonnethead shark, *Sphyrna tiburo*. *Environ Biol Fishes*. 1993;38:25-35.
40. Duboule D. Temporal colinearity and the phylotypic progression: a basis for the stability of a vertebrate Bauplan and the evolution of morphologies through heterochrony. *Development*. 1994;1994-(Supplement):135-142. doi:10.1242/dev.1994.Supplement.135
41. Irie N, Kuratani S. The developmental hourglass model: a predictor of the basic body plan? *Development*. 2014;141(24):4649-4655. doi:10.1242/dev.107318
42. Gabner S, Böck P, Fink D, Glösmann M, Handschuh S. The visible skeleton 2.0: phenotyping of cartilage and bone in fixed vertebrate embryos and foetuses based on X-ray microCT. *Development*. 2020;147(11):dev187633. doi:10.1242/dev.187633
43. Dingerkus G, Uhler LD. Enzyme clearing of Alcian blue stained whole small vertebrates for demonstration of cartilage. *Stain Technol*. 1977;52(4):229-232. doi:10.3109/10520297709116780

How to cite this article: Byrum SR, Frazier BS, Grubbs RD, Naylor GJP, Fraser GJ. Embryonic development in the bonnethead (*Sphyrna tiburo)*, a viviparous hammerhead shark. *Developmental Dynamics*. 2023;1-12. doi:10.1002/dvdy.658